Environmental Toxicology and Chemistry—Volume 40, Number 1—pp. 88–99, 2021
Received: 17 July 2020 | Revised: 11 August 2020 | Accepted: 16 October 2020

Environmental Chemistry

Storm Event–Driven Occurrence and Transport of Dissolved and Sorbed Organic Micropollutants and Associated Effects in the Ammer River, Southwestern Germany

Maximilian E. Müller,[a] Christian Zwiener,[a] and Beate I. Escher[a,b,*]

[a]Center for Applied Geoscience, Eberhard Karls University of Tübingen, Tübingen, Germany
[b]Department of Cell Toxicology, UFZ–Helmholtz Centre for Environmental Research, Leipzig, Germany

Abstract: Storm events lead to agricultural and urban runoff, to mobilization of contaminated particulate matter, and to input from combined sewer overflows into rivers. We conducted time-resolved sampling during a storm event at the Ammer River, southwest Germany, which is representative of small river systems in densely populated areas with a temperate climate. Suspended particulate matter (SPM) and water from 2 sampling sites were separately analyzed by a multi-analyte liquid chromatography–tandem mass spectrometry (LC–MS/MS) method for 97 environmentally relevant organic micropollutants and with 2 in vitro bioassays. Oxidative stress response (AREc32) may become activated by various stressors covering a broad range of physicochemical properties and induction of aryl hydrocarbon receptor–chemical-activated luciferase gene expression (AhR-CALUX) by hydrophobic compounds such as dioxins and dioxin-like molecules. Compound numbers, concentrations, their mass fluxes, and associated effect fluxes increased substantially during the storm event. Micropollutants detected in water and on SPM pointed toward inputs from combined sewer overflow (e.g., caffeine, paracetamol), urban runoff (e.g., mecoprop, terbutryn), and agricultural areas (e.g., azoxystrobin, bentazone). Particle-facilitated transport of triphenylphosphate and tris(1-chloro-2-propyl) phosphate accounted for up to 34 and 33% of the total mass flux even though SPM concentrations were <1 g L^{-1}. Effect fluxes attributed to SPM were similar or higher than in the water phase. The important role of SPM-bound transport emphasizes the need to consider not only concentrations but also mass and effect fluxes for surface water quality assessment and wastewater/stormwater treatment options. *Environ Toxicol Chem* 2021;40:88–99. © 2020 The Authors. *Environmental Toxicology and Chemistry* published by Wiley Periodicals LLC on behalf of SETAC.

Keywords: Storm event; Organic micropollutants; Chemical analysis; In vitro bioassays; Water quality

INTRODUCTION

More and more anthropogenic organic compounds are being used in a broad range of applications and have become indispensable to our modern society. Because of high usage and consumption, they are regularly found in the aquatic environment (Casado et al. 2019; Bradley et al. 2020). Due to their use-specific properties, such as high persistence of flame retardants or effects of pesticides and pharmaceuticals on biological organisms (Daughton and Ternes 1999), they may pose a hazard to ecosystems and drinking water quality (Alpizar et al. 2019; European Environment Agency 2019). Ideally, pharmaceuticals and personal care products are collected after application and managed by municipal sewers and wastewater treatment systems. Other compounds such as pesticides are directly dispersed in agriculture and urban environments. Biocides, used to preserve outdoor materials, facades, and roofs, may leach and be flushed into surface waters by rainfall (Berenzen et al. 2005; Tran et al. 2019; Spahr et al. 2020).

The chemical status of surface waters is generally only assessed by snapshots of individual compound concentrations in regulatory monitoring (Brack et al. 2018). The water quality of small river systems can be highly dynamic (Jordan and Cassidy 2011), and as a recent study on 128 cumulative water samples

This article includes online-only Supplemental Data.

* Address correspondence to beate.escher@ufz.de
Published online 20 October 2020 in Wiley Online Library (wileyonlinelibrary.com).
DOI: 10.1002/etc.4910

taken during rain events at 44 different small streams in Germany demonstrated, each rain event showed a different chemical and effect profile (Neale et al. 2020). Depending on their physicochemical properties, organic micropollutants can sorb to organic carbon or mineral surfaces of soils and sediments (Schwarzenbach et al. 2016). Micropollutant-loaded soil or sediment particles may be released and suspended in rivers during storm events. With increased river discharge during storms, suspended particulate matter (SPM) represents a potential transport vector of organic micropollutants in rivers (Gasperi et al. 2009; Lepom et al. 2009; da Silva et al. 2011; Zgheib et al. 2011; Boulard et al. 2019). Storm and flood events can cause combined sewer overflows and thereby the release of untreated wastewater, including sewage sludge particles, into surface waters (Phillips et al. 2012; Madoux-Humery et al. 2013). Furthermore, remobilization of contaminants from sediments has to be considered (Eggleton and Thomas 2004; de Weert et al. 2010; Müller et al. 2019).

We investigated the impact of a storm event on the concentrations and mass fluxes of dissolved and particle-associated micropollutants and their associated effects, in high temporal resolution at 2 sampling sites at the Ammer River in southwest Germany. Water and SPM were analyzed separately by liquid chromatography–mass spectrometry (LC–MS) and 2 in vitro bioassays. The chemical analysis targeted 97 environmentally relevant organic micropollutants including 45 pesticides, 31 pharmaceuticals, 12 industrial and household chemicals, and 9 other compounds, that have been found regularly in surface waters (Ruff et al. 2015; Casado et al. 2019; van Gils et al. 2020). Mixture effects of all chemicals in water and SPM were quantified with 2 in vitro bioassays that cover the environmentally relevant modes of action of aryl hydrocarbon receptor (AhR) induction and oxidative stress response. Induction of AhR may be activated by hydrophobic compounds such as dioxins and dioxin-like molecules (i.e., planar polychlorinated biphenyls, polychlorinated dibenzodioxins, and dibenzofurans), but also by polycyclic aromatic hydrocarbons; the assay is commonly used to assess sediment quality and the bioavailability and toxicity of sediment-associated contaminants (Li et al. 2013; Eichbaum et al. 2014; Bräunig et al. 2016). Oxidative stress response is induced by a broad range of stressors and has been used for sediment and water quality assessment (Escher et al. 2012; Li et al. 2013; Bräunig et al. 2016).

In the present study we addressed the following questions: 1) What are the dynamics of the total organic micropollutant and effect fluxes in a river during a storm event? 2) How much does SPM-facilitated transport contribute to the total flux of micropollutants and bioactive mixtures? and 3) What is the concentration ratio between water and SPM for micropollutants and effects and does it change during the event?

MATERIALS AND METHODS

Sampling

In the night of 27 July 2019, from 18:30 to 22:45 (all times given as Central European Summer Time, Coordinated Universal Time [UTC] + 2 h) a thunder cell came from the southwest and passed the upper Ammer catchment with precipitation up to 80 mm h^{-1} (Supplemental Data, Figure S1). The precipitation sum for 27 July 2019 was 29 mm at the meteorological station in Herrenberg/Gäufelden, Germany (Baden-Württemberg State Institute for the Environment, Survey and Nature Conservation 2020b). With a discharge maximum of 8772 L s^{-1} at autosampler (AS) AS2 (gauge station in Pfäffingen, Germany) the investigated storm event almost reached the German classification of a biennial flood HQ2 (HQ2: ≥ 11 650 L s^{-1} at the gauge station in Pfäffingen; Baden-Württemberg State Institute for the Environment, Survey and Nature Conservation 2020a). At 2 sampling sites (AS1 and AS2) at the Ammer River, which were located upstream and downstream of a wastewater treatment plant (WWTP1, 80 000 person equivalents, annual mean flow: 100–120 L s^{-1}) and 7.7 km apart, 1 L of river water was sampled every 30 min for a total period of 6 h using ISCO 3700 autosamplers (Teledyne ISCO; Figure 1). The first samples taken at AS1 (AS1_1 at 20:09) and at AS2 (AS2_1 at 21:03) were set as origins (0 h) of the respective time scales (time [h]). A second smaller WWTP (WWTP2, annual mean flow: 12–15 L s^{-1}) with 9000 person equivalents discharges into the Kochart Creek, a tributary of the Ammer River upstream of AS2.

After 14 h, when discharge decreased toward base flow conditions, 1 L of river water was collected at each sampling site. The AS2 samples were taken 53 min after the AS1 samples to capture full hydrographs of both sampling sites. All samples were kept cool at 4 °C and processed within the next 48 h. At AS1 and AS2, discharges were derived from measured water levels (using online probes from UIT) and pre-established rating curves. Discharges (Q) of 15-min intervals (Supplemental Data, Table S1) and amounts of SPM (Supplemental Data, Table S2) have been reported by Glaser et al. (2020). The SPM amounts were derived by filtering (250 mL of replicate samples, 1.5-µm cellulose membrane) according to the German industrial standard Deutsche Industrienorm 38409-2 (1987). At both sampling sites sampling and discharge measurements were not performed at the exact same time. Therefore, the discharge corresponding to a given sample of AS1 was estimated by linear interpolation between the 2 adjacent samples. The discharge for a given sample of AS2 referred to the closest discharge measurement (Supplemental Data, Table S3). The SPM fluxes ($kg_{dry\ weight}\ s^{-1}$) were determined as the SPM amount (Supplemental Data, Table S2) times the discharge (Supplemental Data, Table S3).

Chemicals and reagents

All solvents used were LC–MS grade. Acetonitrile was purchased from Honeywell Riedel-de Haen™. Methanol (Optima®) and water (Optima®) were obtained from Thermo Fisher Scientific. Ethyl acetate was purchased from Acros Organics, Thermo Fisher Scientific. Acetone (SupraSolv®) was obtained from Merck. A list of all analytical standards is given in the Supplemental Data, Table S4.

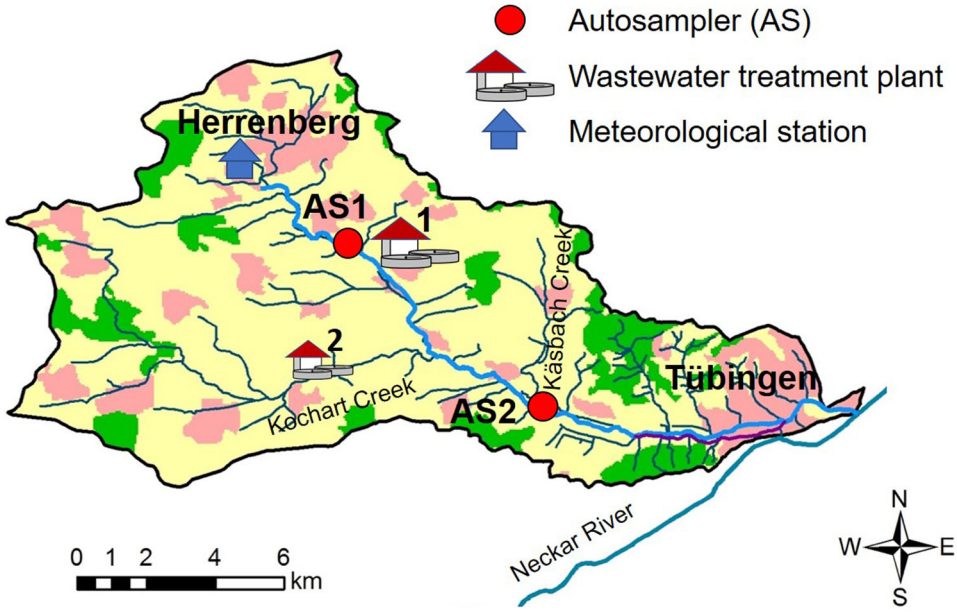

FIGURE 1: Study site in the Ammer catchment near Tübingen, Germany. At 2 sampling sites, autosamplers (AS) AS1 and AS2 (red dots) were installed, and run during the storm event. AS2 was located at the river water gauge station in Pfäffingen. Wastewater treatment plants are located at the Ammer main stem downstream of AS1 (WWTP1, 80 000 PE) and at the Kochart Creek (WWTP2, 9000 PE). The meteorological station (blue house symbol) is located upstream of AS1. The Ammer main stem is highlighted in light blue. Land uses are illustrated in yellow for agriculture, pink for urban areas, and green for forestry. Figure adapted from Müller et al. (2018).

Sample preparation

Accelerated solvent extraction. The SPM from 1 L of river water was separated from the water phase using a cellulose filter (Whatman 595 1/2, pore size: 4–7 µm), frozen at –20 °C overnight, and then freeze-dried for 24 h (Alpha 1-4 LSCplus freeze drier; Martin Christ). Freeze-dried cellulose filters with attached SPM were extracted by accelerated solvent extraction (ASE; Dionex ASE 300 system, Thermo Fisher Scientific). Extraction was performed with acetone:ethyl acetate (50:50, v/v) in 2 cycles, each with 5-min preheat, 10-min static time at 80 °C and 100 bar, a flush volume of 60%, and a purge time of 60 s. More information is provided in the Supplemental Data, S1. The ASE blanks were derived by extracting freeze-dried cellulose filters. The ASE extracts were evaporated to dryness using a rotary evaporator (Rotapovator® R-215; Büchi) and reconstituted with 1 mL methanol. The exact final volumes were determined gravimetrically.

Solid phase extraction. First, 1 L of filtered river water samples was preconcentrated by a factor of 2000 by solid phase extraction (SPE) using cartridges with 200 mg hydrophilic–lipophilic balanced material (Oasis HLB 6 cc; Waters). Further information is provided in the Supplemental Data, S1. For SPE blanks, pure water was used. Finally, all water and SPM extracts, blanks, and samples for assessing extraction recoveries were filtered with a polyethersulfone 0.2-µm filter (Agilent Captiva Premium Syringe filter), to avoid clogging of the high-performance liquid chromatography (HPLC) system, and stored at –20 °C until measurement. Exact volumes of all extracts were determined gravimetrically.

ASE and SPE recoveries

Uncertainty systematically arising from the sample preparation was considered in the result reported (Barwick and Ellison 2000; Cordeiro et al. 2018; Mateos et al. 2020). Therefore, with respect to the absence of sufficient sample volume and the avoidance of internal standards that would lead to signal interference in the bioassays, ASE recovery was assessed by extracting cellulose filters spiked with standard solutions (50 µL of 100 µg L^{-1}, $n = 3$). The SPE recoveries were determined with pure water (Milli-Q) spiked with a standard mix including all target compounds (5 ng L^{-1}, $n = 3$). It was assumed that the systematic analyte loss during SPE and ASE was constant throughout the samples and not affected by the sample matrix.

Chemical analysis

Analyte separation was achieved by a 1260 Infinity HPLC device (Agilent Technologies) using a Poroshell 120 EC-C18 column (2.7-µm particle size, 4.6 × 150 mm; Agilent) at 40 °C. Carrier liquids were water with 0.1 mM ammonium acetate and 17.5 mM acetic acid (A) and acetonitrile with 17.5 mM acetic acid (B). Chromatographic separation was performed with the following gradient program: 0 to 17 min, 95 to 20% A, 17 to 23 min 0% A, 23 to 33 min 95% A. Target screening for 97 target compounds was performed by tandem mass spectrometry (MS/MS; 6490 iFunnel triple quadrupole mass spectrometer; Agilent) using electrospray ionization and 2 mass transitions/analyte (Supplemental Data, Table S5). For 11 target compounds, quantification was performed by internal standard

calibration (internal standard spiked to the samples to a concentration of 5 $\mu g\,L^{-1}$, using an Agilent 1260 Infinity Standard Autosampler prior to LC–MS/MS measurement). For all other target compounds, external standard calibration (9-point calibration) was applied.

Matrix effects were assessed in representative samples by standard addition and 2 concentration levels (0.83 and 3.33 $\mu g\,L^{-1}$, $n = 1$; Supplemental Data, S1 and Table S6). Because the average relative standard deviation of all target compounds (Supplemental Data, Table S8) was 7%, correction for matrix effects of the quantitative results (Supplemental Data, Table S7) was deemed appropriate if the signal suppression or enhancement was outside a range of ±20%. The limit of quantification (LOQ) was defined as the lowest calibration level for which the signal-to-noise ratio was ≥10 and for which the quantifier-to-qualifier ratio was within ±20% of the average ratio of analytical standards. If an analyte was detected in the blank, the 5-fold blank concentration was used as the LOQ. Prior to LC–MS/MS measurements, water extracts were diluted 1:50 in methanol:water (30:70 v/v) to reduce matrix effects (Villagrasa et al. 2007; Kruve et al. 2009). The relative standard deviations of ASE and SPE recoveries of all target compounds were on average 11 and 29%, respectively. Only concentrations of analytes with recoveries <70% were corrected (Supplemental Data, Table S8). Analytes with recoveries <20% were not further considered. Recoveries of acesulfame, citalopram, fluoxetin, and gabapentin were <20%, and these compounds were therefore omitted from further analysis. The relative standard deviations of replicate LC–MS measurements, of a standard solution at 5.0 $\mu g\,L^{-1}$, of each analyte ($n = 10$) are provided in the Supplemental Data, Table S8. In addition, analyte concentrations on SPM were corrected for residual water co-extracted with the SPM filters (Supplemental Data, S1).

Given the available amount of 250-mL sample for determining the SPM concentration (Glaser et al. 2020) and the high uncertainty resulting from subtracting 2 relatively large gravimetric values, we omitted data for compound concentrations in SPM extracts of water sample with SPM concentration <50 $mg_{dry\,weight}\,L^{-1}$ (AS1_12, AS2_1, AS2_2, AS2_3, and AS2_12; Supplemental Data, Table S2) because no reliable and robust results were obtained.

In vitro bioassays

All extracts were tested with 2 in vitro reporter gene bioassays that were indicative for activation of metabolism (activation of aryl hydrocarbon receptor–chemical-activated luciferase gene expression [AhR-CALUX]; Brennan et al. 2015) and activation of oxidative stress response (AREc32; Escher et al. 2012, 2013). Detailed methods are given in König et al. (2017) and Neale et al. (2017). The effect concentration ECIR1.5 (concentration in the assay causing an induction ratio (IR) of 1.5 relative to unexposed cells) for AREc32 and the EC10 (concentration in the assay causing 10% effect relative to 2,3,7,8-tetrachlorodibenzodioxin) for AhR-CALUX were derived based on the linear regression of the lower portion (up to an IR of 4 in AREc32 and up to 30% effect in AhR-CALUX) of the concentration–response curve, according to Escher et al. (2018b). For each bioassay, cell growth inhibition was assessed by measuring the cell area coverage by live cell imaging as described in Escher et al. (2019) and expressed as concentration causing 10% cell growth inhibition (IC10). The ECIR1.5, EC10, and IC10 values of water extracts were expressed as relative enrichment factors (REFs), taking into account the enrichment during the sample preparation procedure and the dilution in the assay. The REFs are in units of $L_w\,L_{bioassay}^{-1}$ for water extracts and $mg_{dry\,weight}\,L_{bioassay}^{-1}$ for SPM extracts. Effect concentrations were then translated into bioanalytical equivalent concentrations (BEQs) by relating the effect of the extract to a reference chemical (Escher et al. 2018a), using Equation 1.

$$\text{BEQ} = \frac{\text{EC10 (reference)}}{\text{EC10 (sample)}} \text{ or } \frac{\text{ECIR1.5 (reference)}}{\text{ECIR1.5 (sample)}} \quad (1)$$

A list of the quality control reference chemicals (tert-butylhydroquinone and 2,3,7,8-tetrachlorodibenzodioxin) and the reference chemicals dichlorvos and benzo[*a*]pyrene (BaP) for derivation of the BEQ (dichlorvos-EQ and BaP-EQ) and their ECs is given in the Supplemental Data, Table S9. Because low effects were detected in the SPE and ASE blanks, the effects of the samples were corrected by blank subtraction ($BEQ = BEQ_{sample} - BEQ_{blank}$). During this process, the effects (BEQ) measured in the SPE and ASE blanks were converted to the matching enrichment factor of the sample. This was necessary because enrichment factors of SPM extracts differed widely, resulting in higher relative background of samples with small SPM amounts. Blanks showed no cytotoxicity in the bioassays. Analogously to the chemicals analysis (Supplemental Data, Equation S1), results of the SPM extracts were corrected for the cytotoxicity using toxic units (Müller et al. 2018) and effects (BEQ) ascribed to the co-extracted water in the SPM filters. Similar to the chemical analysis, we omitted effect data of SPM extracts from samples with SPM concentrations <50 $mg_{dry\,weight}\,L^{-1}$.

Calculation of mass and effect fluxes

Mass fluxes were calculated from analyte concentrations in water ($\mu g\,L^{-1}$) and on SPM ($\mu g\,g_{dry\,weight}^{-1}$) by multiplication with the flow rate Q ($L\,s^{-1}$) and the SPM flux ($g\,s^{-1}$), respectively (Equations 2 and 3).

$$J_{i,water} = Q \times C_{i,water} \quad (2)$$

$$J_{i,SPM} = \text{SPM flux} \times C_{i,SPM} \quad (3)$$

where $J_{i,water}$ is the mass flux in water and $J_{i,SPM}$ is the mass flux attributed to SPM, of compound *i*. The fraction f_{SPM} describes the portion of the total mass flux that was attributed to SPM and was calculated using Equation 4.

$$f_{SPM} = \frac{J_{i,SPM}}{(J_{i,SPM} + J_{i,water})} \quad (4)$$

Bioanalytical effect fluxes (BEFs; mass of reference compound equivalent effect in the respective bioassay/second) were calculated using Equation 5 for water (dichlorvos-BEF_{water} and BaP-BEF_{water}) and Equation 6 for SPM (dichlorvos-BEF_{SPM} and BaP-BEF_{SPM}) from the BEQ measured in water (dichlorvos-EQ_{water} [$\mu g_{dichlorvos}\ L^{-1}$] in AREc32, and BaP-$EQ_{water}$ [$ng_{BaP}\ L^{-1}$] in AhR-CALUX) or SPM extracts (dichlorvos-EQ_{SPM} [$\mu g_{dichlorvos}\ g_{dry\ weight}^{-1}$] in AREc32 and BaP-$EQ_{SPM}$ [$ng_{BaP}\ g_{dry\ weight}^{-1}$] in AhR-CALUX).

$$BEF_{water} = Q \times BEQ_{water} \quad (5)$$

$$BEF_{SPM} = \text{SPM flux} \times BEQ_{SPM} \quad (6)$$

Distribution between micropollutants in water and on SPM

The concentration ratio (R_i in $L\,kg^{-1}$) of a compound i between water and SPM was calculated using Equation 7, based on the compound concentration measured in the water ($C_{i,water}$ in $\mu g\ L^{-1}$) and on SPM ($C_{i,SPM}$ in $\mu g\ kg_{dry\ weight}^{-1}$) extract.

$$R_i = \frac{C_{i,SPM}}{C_{i,water}} \quad (7)$$

The BEQ ratio R_{BEQ} between water and SPM was calculated analogously to Equation 7. Partitioning of a compound i between water and organic carbon of SPM at equilibrium (K_d) was estimated from the octanol/water partition coefficient (K_{OW}), the organic carbon content of SPM, and an empirical correlation from Karickhoff (1981), using Equation 8. This empirical correlation only accounts for hydrophobic compounds that are not ionized and was only applied to compounds that were shown to predominantly partition to the organic carbon of SPM. The organic carbon content (f_{OC}) was derived from the amount of sampled SPM, the dissolved organic carbon (DOC), which refers to organic carbon after 0.45-µm filtration, and the total organic carbon concentration; these data were obtained from replicate samples as reported in Glaser et al. (2020; Supplemental Data, Table S2). The K_{OW} values of target compounds detected in water and SPM extracts are provided in the Supplemental Data, Table S10.

$$K_d = f_{OC} \times K_{OC} = f_{OC} \times 0.41 \times K_{OW} \quad (8)$$

We need to note that the DOC of the water samples was defined as the organic carbon dissolved in water and on particles <0.45 µm. The SPM measured by chemical analysis and bioassays was defined as the particle fraction size in the water samples >4 to 7 µm. The concentration of SPM measured in the water samples was defined as the particle fraction size in the water samples >1.5 µm.

RESULTS AND DISCUSSION

Chemical analysis

Micropollutants in water. At AS1, 27 of 97 target compounds were detected (11 pesticides, 9 pharmaceuticals, and 7 industrial and household chemicals). At AS2, 33 of 97 target compounds were detected (10 pesticides, 17 pharmaceuticals, and 6 industrial and household chemicals), with 25 compounds detected at both sites. Between AS1 and AS2 the compounds perfluorohexanoic acid and propiconazole disappeared, and 8 additional compounds were detected at AS2, along with fluconazole, sotalol, oxcarbazepine, sulfamethoxazole, and trimethoprim. The latter were demonstrably introduced by WWTP1 under dry weather conditions (Müller et al. 2020). Measured concentrations of all target compounds in the water extracts and quantification limits are provided in the Supplemental Data, Tables S11 and S12.

For a better understanding and visualization of the mass flux dynamics and potential input sources, the detected compounds were subdivided into 3 major groups. This division was made on the basis of their mass flux dynamics at AS1 and AS2 (groups 1, 2, and 3; Supplemental Data, Table S13), and thus compounds from different groups showed different courses of mass fluxes over time. Group 1 compounds showed higher or equally high average mass fluxes at AS1 compared with AS2. Group 2 compounds showed 10× higher average mass fluxes at AS2. Group 3 comprised compounds that were detected at AS1 and showed moderately increased average mass fluxes (below a factor of 10) at AS2. One-half of the LOQ was used as a substitute for all samples with concentrations below the LOQ, as recommended by the US Environmental Protection Agency (2000). It is important to note that interpretation of data with nondetects is generally biased (Helsel 1990; Kayhanian et al. 2002). The mass flux dynamics of the 3 groups are shown in Figure 2.

Group 1 compounds were more abundant at AS1 compared with AS2 (Figure 2A and B) and thus were introduced from different input sources of the upper Ammer catchment, such as stormwater from agricultural and urban areas and combined sewer overflows. Storm water input from urban areas is suggested by the biocides carbendazim, diuron, and propiconazole, which are used to preserve outdoor materials and façades. The presence of the plasticizer and flame retardant triphenyl phosphate (TPP) also indicates input from urban areas and wastewater. At AS1, caffeine and paracetamol were detected; both are anthropogenic markers for untreated wastewater (Buerge et al. 2003; Kasprzyk-Hordern et al. 2009). Interestingly, the concentrations of caffeine and paracetamol at AS1 kept increasing throughout the storm event (Supplemental Data, Figure S2A), indicating an increasing portion of untreated wastewater in the Ammer, perhaps through combined sewer overflows.

Many compounds ascribed to group 2 were pharmaceuticals and industrial and household chemicals, which typically find their way into rivers by the route of treated wastewater, indicating a major influence of WWTP1 on the dynamics of group 2 compounds. Indeed, flow measurements showed that WWTP1 released much more water during the storm event. At 20:00 (27 July 2019), the WWTP1 influent substantially increased and exceeded the maximum influent capacity (Supplemental Data, Figure S3), leading to a maximum flow rate of $690\ L\ s^{-1}$ through the WWTP and redirection of the spillover into storm water

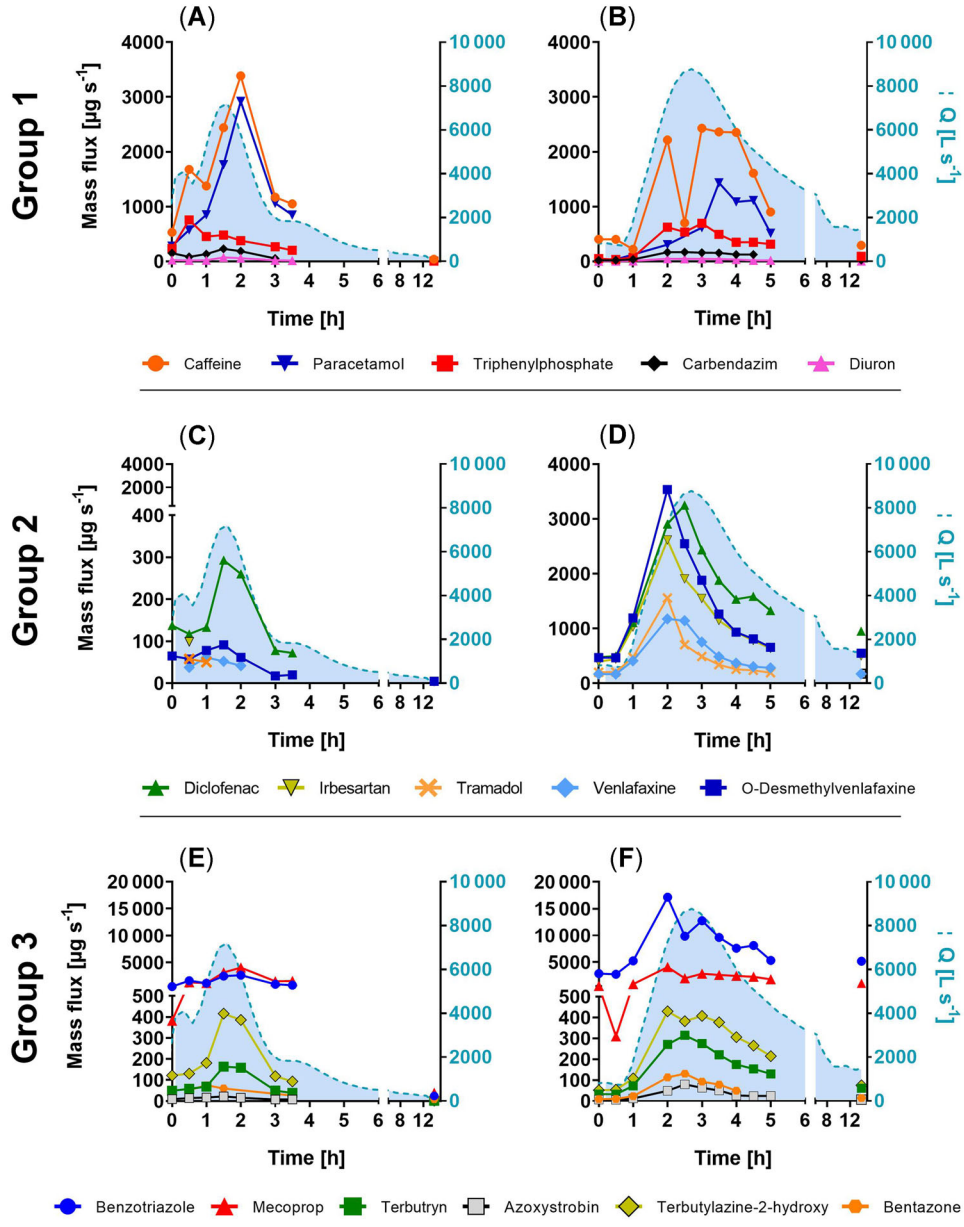

FIGURE 2: Mass fluxes (µg s^{-1}) of selected compounds in water during the storm event that fell into 3 groups. Chemicals in group 1 showed a higher or equally high average mass flux at autosampler (AS) AS1 (**A**) compared with AS2 (**B**). Group 2 showed a 10× higher average mass flux at AS2 (**D**) than at AS1 (**C**). Group 3 chemicals were detected at AS1 (**E**) with moderately increased (below a factor of 10) average mass fluxes compared with AS2 (**F**). Mass fluxes are depicted on the left vertical axis, and discharge is depicted as light blue area and on the right vertical axis. MCPA = (4-chloro-2-methylphenoxy)acetic acid.

retention basins. At AS1, a few pharmaceuticals had already appeared due to input from combined sewer overflows. The mass fluxes of selected compounds at AS1 and AS2 (Figure 2C and D) increased with increasing discharge and roughly followed the hydrograph. Interestingly and considering the concentrations, group 2 compounds at AS2 increased even before the discharge increased (Supplemental Data, Figure S2D). An explanation could be a "first flush" upstream of AS2, that is, contaminated storm water leading to high concentrations in the receiving river, early in the storm hydrograph (Bertrand-Krajewski et al. 1998; Lee et al. 2002; Peter et al. 2020). Similar dynamics were observed by Madoux-Humery et al. (2013) and Phillips et al. (2012), who found generally higher pollutant concentrations in the beginning of storm events when inputs were high and dilution low, which decreased when dilution kicked in.

Compounds of group 3 (Supplemental Data, Table S13) were detected at AS1 and showed moderately increased mass fluxes at AS2, hinting at inputs upstream of AS1 and between AS1 and AS2. The corrosion inhibitor benzotriazole showed the highest mass fluxes of all detected compounds and was likely introduced by a combined sewer overflow and in large amounts by WWTP1. Pesticides commonly applied in agriculture (bentazone, azoxystrobin, mecoprop) and a pesticide

transformation product (terbutylazine-2-hydroxy), pointed toward inputs from agricultural areas. Szöcs et al. (2017) identified agricultural land use as a substantial input source of pesticides in streams and detected a higher number of pesticides following rainfall. Moreover, mecoprop is applied as a biocide against root penetration in bituminous sealings and felts on flat roofs, and terbutryn is used in façade paintings. Rainfall may wash both of them off into surface waters (Bucheli et al. 1998; Burkhardt et al. 2011). Propiconazole (a group 1 compound) was detected at the maximum discharge at AS1. It is used as fungicide in wood preservation and has been found during storm event conditions by other researchers in an urban catchment (Gasperi et al. 2008). Because mecoprop and propiconazole were not detected in the Ammer River under dry weather conditions (Müller et al. 2020), they could potentially be used as storm water indicators in future studies.

Remarkably, the numbers, concentrations, and mass fluxes of the target compounds investigated in the present study were generally higher during the storm event compared with dry weather conditions, according to data from previous studies at the Ammer River in 2017 (Müller et al. 2018) and 2018 (Müller et al. 2020). At base flow, compounds introduced by wastewater and/or from agricultural areas occurred at AS2 in the lower ng L^{-1} range. These compounds showed higher concentrations under storm event conditions by factors of 4 for benzotriazole, 7 for tris(1-chloro-2-propyl) phosphate (TCPP), 3 for 4- and 5-methylbenzotriazole, 3 for carbamazepine, 2 for isoproturon, and 3 for bentazone. The mass fluxes of the same compounds, however, increased by factors of 26 for benzotriazole, 77 for TCPP, 26 for 4- and 5-methylbenzotriazole, 17 for carbamazepine, 15 for isoproturon, and 18 for bentazone during the storm event. The absolute total mass of all compounds (detected then and now) passing AS2 over 12 h was 122 g during the same time period in 2018 and during base flow, but it was 1028 g in the present study, although only 18 compounds were detected then, and now we can estimate a pollutant load difference of 1 order of magnitude between dry and wet weather conditions. Moreover, in 2017 and 2018, 9 and 15 of the now detected compounds were in concentrations below the limit of detection. Thus, during the investigated storm event, micropollutant numbers and concentrations increased considerably along with a generally even more pronounced mass flux increase.

Micropollutants sorbed to SPM. The compounds isoproturon, tebuconazole, and terbutryn were found in the majority of the SPM samples. Highest concentrations were found for the organophosphates TPP, TCPP, and tris(2-butoxyethyl) phosphate (TBEP; Supplemental Data, Tables S14 and S15). In total 16 compounds, comprising 10 pesticides, 2 pharmaceuticals, and 4 industrial and household chemicals, were detected in the SPM extracts. Fenofibrate, azoxystrobin, and carbendazim were exclusively detected in SPM extracts of AS1 and perfluorooctanesulfonic acid (PFOS), atrazine, and prochloraz exclusively in SPM extracts of AS2. The SPM fluxes in the Ammer River followed the hydrographs at AS1 and AS2 and were at maximum 7.10 and 2.93 $kg_{dry\ weight}$ s^{-1} (after 1.5 and 3.4 h, respectively; Supplemental Data, Table S3). Glaser et al. (2020) found a broader discharge function at AS2 and a particle loss of approximately 13% between both sampling sites. Again, the target compounds detected in the SPM extracts from AS1 and AS2 can be subdivided into 3 groups in terms of the mass flux dynamics associated with SPM, similar to the compounds detected in the water extracts. In this case, only compounds detected 3 times in a row were considered.

Among the group 1 compounds, which showed higher or equally high average particle-associated mass fluxes at AS1 compared with AS2, was TPP (Figure 3), a typical wastewater pollutant widely used as a plasticizer and flame retardant (Meyer and Bester 2004; Kim et al. 2017). The presence of TPP points toward micropollutant input from a combined sewer overflow upstream of AS1, as already suggested by organic indicator chemicals (caffeine and paracetamol) in the water samples from AS1. Diflufenican is a pesticide commonly used in agriculture, and isoproturon is a biocide used in domestic

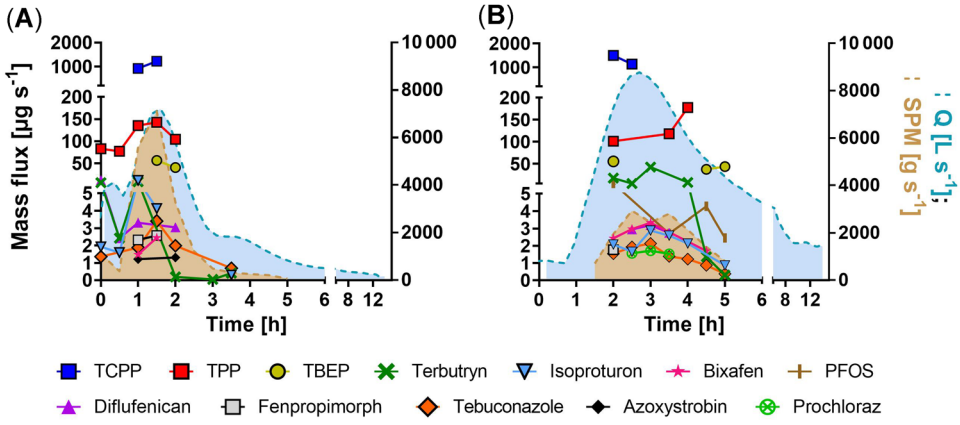

FIGURE 3: Mass fluxes associated with suspended particulate matter (µg s^{-1}) of detected compounds at the autosamplers (AS) AS1 (**A**) and AS2 (**B**) over time. Mass fluxes are depicted on the left vertical axis, and discharge and suspended particulate matter (SPM) flux are depicted on the right vertical axis as light blue and light brown areas. TCPP = tris(1-chloro-2-propyl) phosphate; TPP = triphenylphosphate; TBEP = tris(2-butoxyethyl) phosphate; PFOS = perfluorooctanesulfonic acid.

applications. This suggests inputs from agricultural and from urban areas.

Prochloraz, assigned to group 2, is used as fungicide in agriculture and could thus come from inputs of agricultural areas between AS1 and AS2, for instance, through the agriculturally impacted Käsbach Creek (Figure 1; Müller et al. 2020).

In group 3 the fungicides bixafen and tebuconazole and the biocide terbutryn were detected, which points to agricultural (bixafen) and urban input (tebuconzole, terbutryn).

Among all detected compounds, azoxystrobin, isoproturon, terbutryn, TPP, TCPP, and TBEP were found in, both water and SPM. A comparison of the mass fluxes in water and SPM of these compounds revealed dominant transport in water. The portion of the total mass fluxes attributed to SPM was at maximum 34% for TPP and TCPP at AS2 (Figure 4). For the organophosphate TBEP and the herbicide isoproturon, up to 15% of the total mass flux was attributed to SPM.

The log K_{OW} is 2.8 for isoproturon and TCPP, and >4 for azoxystrobin, TPP, and TBEP (Supplemental Data, Table S10). These compounds are neutral at pH 7.4 and predominantly partition to the organic carbon of SPM (Worrall et al. 1996; Kodešová et al. 2011; Kim et al. 2017). The comparison between the measured concentration ratios R_i between SPM and water (Equation 7) and the predicted partition coefficient K_d (Equation 8) depicted in Figure 5, gives an estimate of whether equilibrium was reached. For TPP, TBEP, and isoproturon at AS1 and AS2, the R_i agreed well with the K_d estimated on the basis of K_{OW}. Because environmental parameters and conditions in rivers (such as DOC and particle and ion concentrations) may change very quickly during storm events, it is all the more surprising that the results indicate that SPM and water could be equilibrated. An R_i 11 to 29 times higher than K_d was observed for TCPP, indicating particle-associated input of TCPP from particles with higher concentrations than found in the Ammer River. Azoxystrobin occurred at R_i 47 and 18 times lower than K_d. Therefore, input of azoxystrobin via the dissolved phase could be linked to direct agricultural application, especially because it was only found in AS1. However, this comparison should be considered with caution because chemicals sorbed to small particles below the applied filter cutoff of 4 to 7 μm would be attributed to the water phase. The fitting factor of 0.41 used in this approximation, empirically determined by Karickhoff (1981), might not apply to all compounds.

All compounds detected in the SPM extracts have log K_{OW} values >1.5. These compounds, except for fenpropimorph and PFOS, are not charged at pH 7.4 (Supplemental Data,

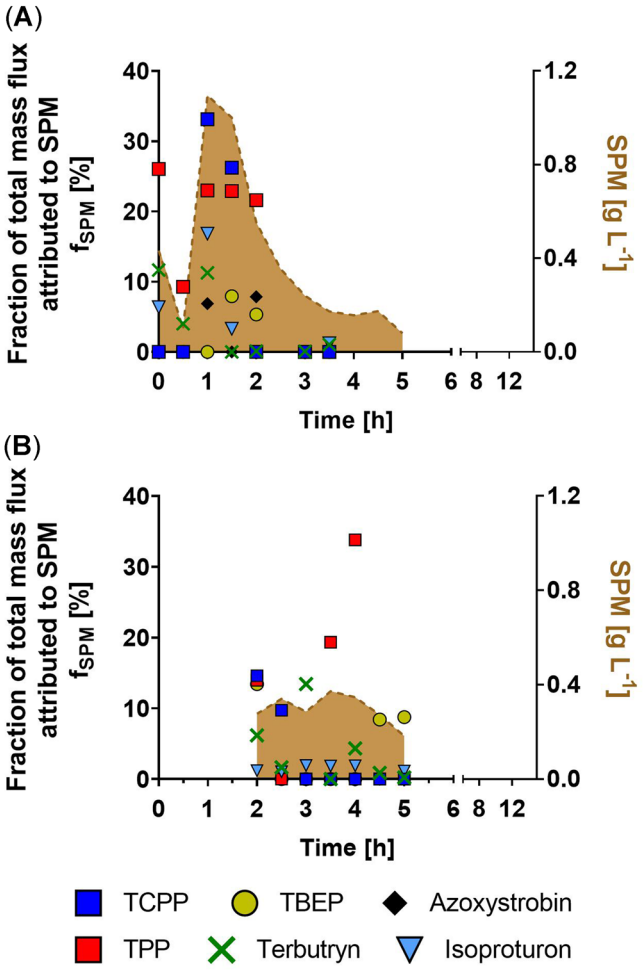

FIGURE 4: Fraction of the total mass flux attributed to suspended particulate matter (f_{SPM}; Equation 4) at the autosamplers (AS) AS1 (**A**) and AS2 (**B**) of compounds detected in water and SPM extracts. TCPP = tris(1-chloro-2-propyl) phosphate; TPP = triphenylphosphate; TBEP = tris(2-butoxyethyl) phosphate.

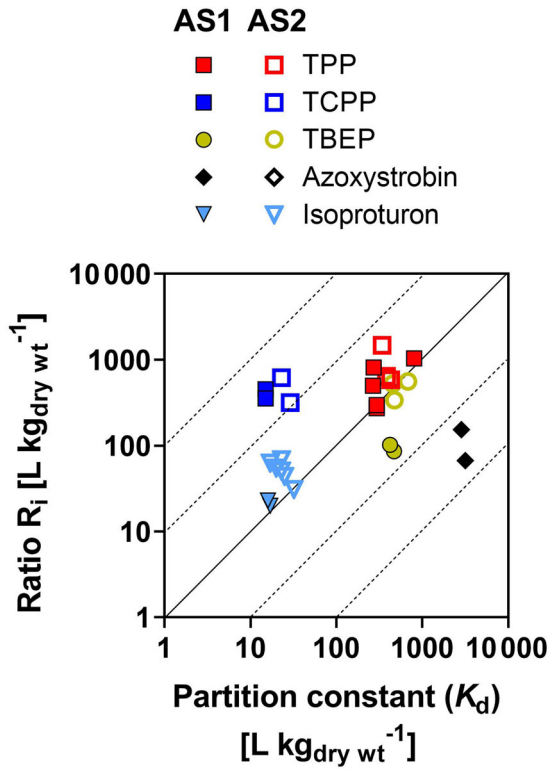

FIGURE 5: Observed concentration ratio (R_i in L kg^{-1}; Equation 7) versus the partition constant (K_d; Equation 8) between water and organic carbon of suspended particulate matter (SPM) during the storm event, for the compounds azoxystrobin, isoproturon, TPP (triphenylphosphate), TBEP (tris(2-butoxyethyl) phosphate), and TCPP (tris(1-chloro-2-propyl) phosphate), at the autosamplers (AS) AS1 (filled symbols) and AS2 (empty symbols).

Table S10) and partition predominantly to the organic carbon of SPM. Fenpropimorph is positively and PFOS negatively charged at pH 7.4, and sorption would not be expected to partition to organic carbon but rather bind via electrostatic attraction to oppositely charged surface sites.

In vitro bioassays

During the storm event the BEQs measured in the SPM extracts (Supplemental Data, Table S17) from AS1 in the AREc32 assay showed variability that increased toward the end of the event (Figure 6A). The BEQs in SPM extracts from AS2 stayed level before they also increased in the last 2 samples (Figure 6B). The BEQs measured in the water extracts were fairly constant, with coefficients of variation of only 32% at AS1 and 34% at AS2 (Figure 6A and B).

The effect distribution ratio R_{BEQ} of effects measured in the water and SPM extracts, from AS1 and AS2, varied between 1000 and 10 000 (Supplemental Data, Figure S4), indicating that most of the chemicals responsible for the measured effects were associated with SPM. The BEF associated with SPM, BEF_{SPM}, was as large or even larger than the BEF associated with water, BEF_{water}, at AS1 and AS2, despite the 1000 times lower mass of SPM than water (Figure 6C and D). The BEF_{water} followed the discharge with a delay of 0.5 h at AS1 (Figure 6C) and 1.5 h at AS2 (Figure 6D). Both BEF_{SPM} and BEF_{water} increased during the storm event at both sampling sites. At AS1, BEF_{SPM} was higher than BEF_{water} after 1 to 2 h, and then both went down parallel with Q. Both BEF_{SPM} and BEF_{water} increased by 3- and 2-fold at AS1 and by 26- and 8-fold at AS2 during the storm event (first sample compared with the sample taken at highest discharge). At both sampling sites the BEF_{SPM} followed the SPM flux.

In the AhR-CALUX assay, the BEQs in water and SPM (Supplemental Data, Table S18) at AS1 followed the water and SPM discharge during the storm event (Figure 7A). At AS2, effects in water increased following the discharge, with a 2-h delay, similar to that shown by AREc32 (Figure 7B). Most of the chemicals responsible for the effects in AhR-CALUX partitioned onto SPM, as revealed by the distribution ratio R_{BEQ} of effects measured in the water and SPM extracts from AS1 and AS2, which varied between 1000 and 100 000 (Supplemental Data, Figure S4). As a consequence, the BEF_{SPM} was generally higher than the associated BEF_{water}, although the SPM mass was approximately 1000 times smaller than the water. Similar to the AREc32 assay, the BEF_{SPM} and water BEF_{water} increased during the storm event at AS1 and AS2 in the AhR-CALUX assay (Figure 7C and D). Both BEF_{SPM} and BEF_{water} at AS1 were much higher than at AS2, in line with the SPM flux.

In 29 and 59% of the samples taken during the actual storm event, the major portion of effects in AREc32 and AhR-CALUX were transported via SPM. The distribution ratios R_{BEQ} of effects measured in the water and SPM extracts in AhR-CALUX and AREc32 were similar, being distribution constants between surface water and sediments, as determined by Bräunig et al. (2016), who investigated the same endpoints. Bräunig et al. (2016) measured higher distribution ratios in bed sediments of larger rivers and estuaries. In the present study, the BEQ_{water} values measured in water in AhR-CALUX were approximately 10 times higher than in 2018 (Müller et al. 2020), under dry weather conditions and in the same river section. In 2018 no or low effects were detected by AREc32.

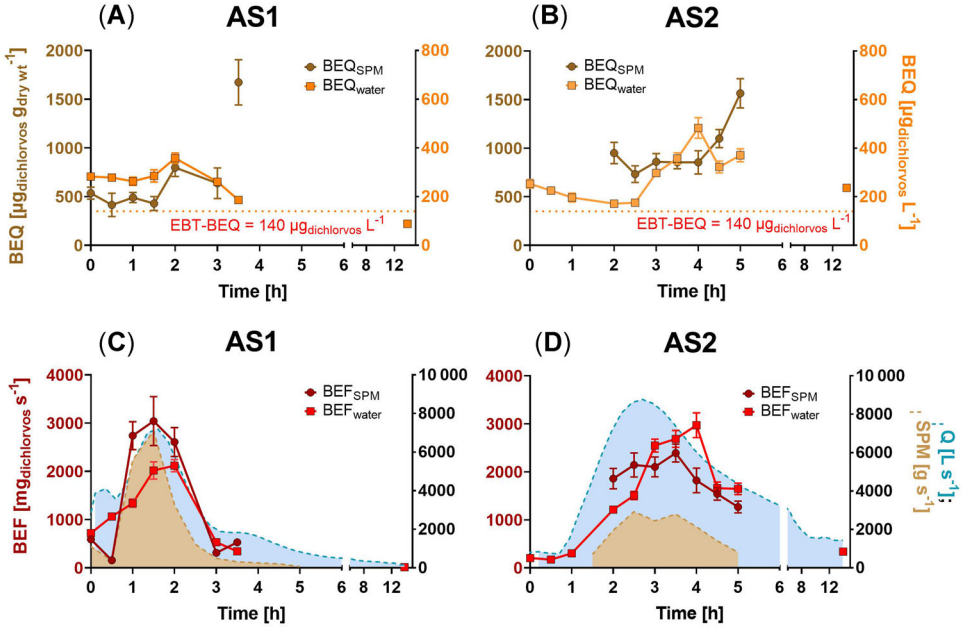

FIGURE 6: The time course of the bioanalytical equivalent concentrations (BEQs), specifically dichlorvos-EQ, in the AREc32 assay of extracted suspended particulate matter (BEQ_{SPM}) and water (BEQ_{water}) at the autosamplers (AS) AS1 (**A**) and AS2 (**B**) and bioanalytical effect fluxes (BEFs) in AREc32 associated with BEF_{SPM} and water (BEF_{water}) compared with discharge Q and SPM flux on the second vertical axis, at AS1 (**C**) and AS2 (**D**). The effect-based trigger value (EBT-EQ) for the oxidative stress response in AREc32, updated by Neale et al. (2020), is visualized by a dotted line. Error bars indicate standard errors.

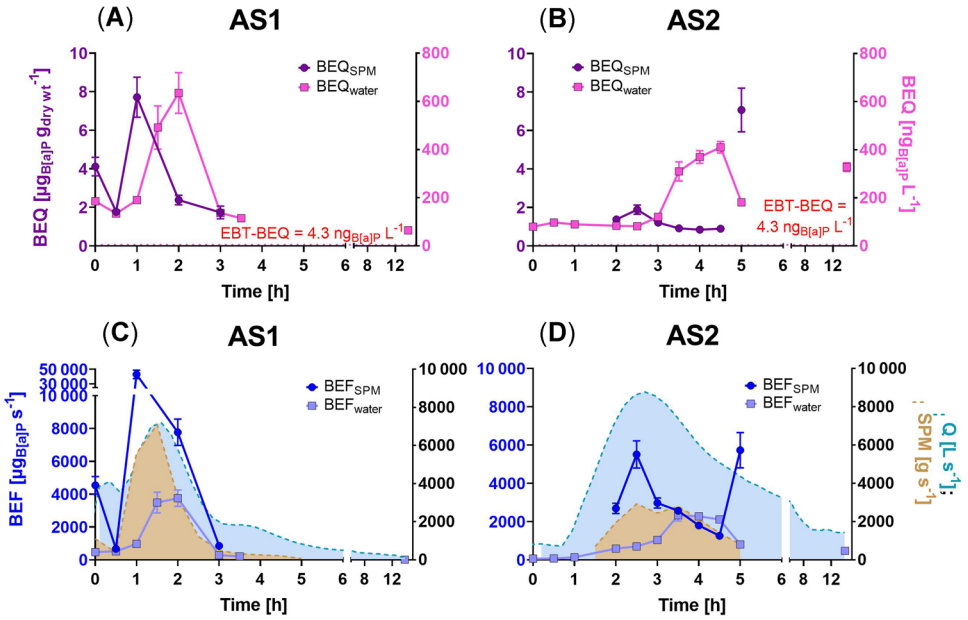

FIGURE 7: Time course of the bioanalytical equivalent concentration (BEQ), specifically benzo[*a*]pyrene-EQ, in the aryl hydrocarbon receptor (AhR–chemical-activated luciferase gene expression [AhR-CALUX]) of extracted suspended particulate matter (BEQ_{SPM}) and water (BEQ_{water}) at the autosamplers (AS) AS1 (**A**) and AS2 (**B**) and bioanalytical effect fluxes (BEFs) associated with BEF_{SPM} and water (BEF_{water}) compared with discharge *Q* and SPM flux on the second vertical axis, at AS1 (**C**) and AS2 (**D**). The effect-based trigger value (EBT-EQ) for AhR-CALUX, updated by Neale et al. (2020), is visualized by a dotted line. Error bars indicate standard errors.

Neale et al. (2020) performed an automated sampling of water at 44 sites in small German rivers, mostly influenced by agriculture and/or wastewater, triggered by rain events. They found a high spatial and temporal variability of the chemical and effect profile in water. Although the majority of samples showed lower effects in AhR-CALUX compared with the present study, the effects measured in AREc32 were in the same range in both studies. The bioassay data of the water extracts from AS1 and AS2 were further compared with tentative effect-based trigger values (EBT-BEQ; Escher et al. 2018a), which were derived from environmental quality standards of the European Union and can serve as effect thresholds indicating poor water quality if exceeded. The EBT-dichlorvos-EQ is 140 $\mu g_{dichlorvos}\ L^{-1}$ for AhR-CALUX, and the EBT-EQ for BaP is 4.3 $ng_{benzo[a]pyrene}\ L^{-1}$ for AREc32, as updated by Neale et al. (2020) using newly available single chemical effect data. The EBT-EQs were exceeded in AREc32 in all samples, except for AS1_12 (13.9 h at AS1) when discharge had returned to base flow after the storm event. Exceedance of EBT-EQ was much more pronounced for AhR-CALUX, pointing toward overall poor water quality with respect to these mixture effect endpoints.

In summary, the bioactive pollutants captured by the bioassays increased much more during the storm event than the individual chemicals analyzed. During the storm event, the BEFs attributed to SPM were as high or even higher than the BEFs attributed to water.

CONCLUSIONS

Storm events pose hazards to the aquatic environment. Numbers of micropollutants, concentrations, mass fluxes, and associated effects and effect fluxes substantially increased during the investigated storm event. Water and SPM originated from combined sewer overflow, urban and agricultural areas, and treated wastewater, with complex contributions that could not completely be traced back to the sources without detailed information on their origin. Water and SPM are inextricably intertwined and exchange organic micropollutants; some neutral compounds appear to occur in concentration ratios close to thermodynamic equilibrium. The SPM turned out to play a particularly important role in the transport of bioactive organic micropollutants, as demonstrated by the dominance of effect flux on SPM over water. The mixture effects of chemicals associated with SPM do not mean that these chemicals are bioavailable. We used the bioassays only to capture complex mixtures, not to form any conclusions with respect to organisms that ingest particles.

Further research would be necessary on whether these pollutants were transported into the Ammer River by particles flushed in during the storm event or whether they originated from mobilized riverbed sediment. For polycyclic aromatic hydrocarbons, it was shown that they rather stemmed from remobilized river sediment during the same event (Glaser et al. 2020), but the sources could be entirely different for the pesticides, consumer products, and pharmaceuticals we investigated.

Despite the much smaller mass contribution of SPM than water, effects and effect flux equivalents attributed to SPM were as high as or even higher than in the water phase. Our study emphasizes that micropollutant inputs triggered by storm events represent an important portion of the overall chemical load in a river. Further research should thus focus on elucidating the impact of different hydrological conditions on the

overall chemical load in a river and assessing their long-term influence on the aquatic environment. Furthermore, particle-facilitated transport of micropollutants, particularly those that may cause toxicity, cannot be neglected in terms of surface water quality monitoring and management.

Supplemental Data—The Supplemental Data are available on the Wiley Online Library at https://doi.org/10.1002/etc.4910.

Acknowledgment—The authors thank C. Zarfl, C. Glaser and M. Schwientek for their help in planning and conducting the sampling, S. Novak for her assistance with sample preparation in Tübingen, and M. König and R. Schlichting for performing the bioassays. We gratefully acknowledge access to the platform CITEPro (Chemicals in the Terrestrial Environment Profiler) funded by the Helmholtz Association. The present study was supported by the Collaborative Research Centre 1253 CAMPOS (Project P1: Rivers), funded by the German Research Foundation (grant SFB 1253/1 2017). Open access funding enabled and organized by Projekt DEAL.

Disclaimer—All authors have no interest to declare. The views expressed in the present study are solely those of the authors.

Author Contributions Statement—M.E. Müller planned and conducted the sampling, sample preparation, chemical analysis, and evaluation and interpretation of the data, wrote the manuscript, and created the initial design of all figures. C. Zwiener planned the sampling, made substantial contributions to the chemical analysis and interpretation of data, and revised the manuscript. B.I. Escher designed the sampling, developed all the bioassay methods and effect-based trigger values, supervised the bioassay measurements, analysis, and interpretation of data, and revised the manuscript.

Data Availability Statement—Data, associated metadata, and calculation tools are available from the corresponding author (beate.escher@ufz.de).

REFERENCES

Alpizar F, Backhaus T, Decker N, Eilks I, Escobar-Pemberthy N, Fantke P, Geiser K, Ivanova M, Jolliet O, Kim H-S. 2019. UN Environment Global Chemicals Outlook II—From legacies to innovative solutions: Implementing the 2030 agenda for sustainable development. United Nations, Geneva, Switzerland.

Baden-Württemberg State Institute for the Environment, Survey and Nature Conservation. 2020a. Daten- und Kartendienst der LUBW. Karlsruhe, Germany. [cited 2020 May 15]. Available from: https://udo.lubw.baden-wuerttemberg.de/projekte/api/processingChain?ssid=62abf969-105e-4ab2-8b20-b07c853b14d6&selector=abflussBW.Hochwasser.bwabfl%3Abwabfl_sel_hq_pegel.sel

Baden-Württemberg State Institute for the Environment, Survey and Nature Conservation. 2020b. Hochwasservorhersagezentrale Baden-Württemberg der LUBW. Karlsruhe, Germany. [cited 2020 May 15]. Available from: https://hvz.lubw.baden-wuerttemberg.de/pegel.html?id=00359

Barwick V, Ellison S. 2000. VAM project 3.2.1. Development and harmonization of measurement uncertainty principles. Part (d): Protocol for uncertainty evaluation from validation data. Report no. LGC/VAM/1998/088. LGC, Teddington, UK.

Berenzen N, Lentzen-Godding A, Probst M, Schulz H, Schulz R, Liess M. 2005. A comparison of predicted and measured levels of runoff-related pesticide concentrations in small lowland streams on a landscape level. *Chemosphere* 58:683–691.

Bertrand-Krajewski J-L, Chebbo G, Saget A. 1998. Distribution of pollutant mass vs volume in stormwater discharges and the first flush phenomenon. *Water Res* 32:2341–2356.

Boulard L, Dierkes G, Schlüsener MP, Wick A, Koschorreck J, Ternes TA. 2019. Spatial distribution and temporal trends of pharmaceuticals sorbed to suspended particulate matter of German rivers. *Water Res* 171:115366.

Brack W, Escher BI, Müller E, Schmitt-Jansen M, Schulze T, Slobodnik J, Hollert H. 2018. Towards a holistic and solution-oriented monitoring of chemical status of European water bodies: How to support the EU strategy for a non-toxic environment? *Environ Sci Eur* 30:1–11.

Bradley PM, Journey CA, Button DT, Carlisle DM, Huffman BJ, Qi SL, Romanok KM, Van Metre PC. 2020. Multi-region assessment of pharmaceutical exposures and predicted effects in USA wadeable urban-gradient streams. *PLoS One* 15:e0228214.

Bräunig J, Tang JY, Warne MSJ, Escher BI. 2016. Bioanalytical effect-balance model to determine the bioavailability of organic contaminants in sediments affected by black and natural carbon. *Chemosphere* 156:181–190.

Brennan JC, He G, Tsutsumi T, Zhao J, Wirth E, Fulton MH, Denison MS. 2015. Development of species-specific Ah receptor-responsive third generation CALUX cell lines with enhanced responsiveness and improved detection limits. *Environ Sci Technol* 49:11903–11912.

Bucheli TD, Müller SR, Voegelin A, Schwarzenbach RP. 1998. Bituminous roof sealing membranes as major sources of the herbicide (R, S)-mecoprop in roof runoff waters: Potential contamination of groundwater and surface waters. *Environ Sci Technol* 32:3465–3471.

Buerge IJ, Poiger T, Müller MD, Buser H-R. 2003. Caffeine, an anthropogenic marker for wastewater contamination of surface waters. *Environ Sci Technol* 37:691–700.

Burkhardt M, Zuleeg S, Vonbank R, Schmid P, Hean S, Lamani X, Bester K, Boller M. 2011. Leaching of additives from construction materials to urban storm water runoff. *Water Sci Technol* 63:1974–1982.

Casado J, Brigden K, Santillo D, Johnston P. 2019. Screening of pesticides and veterinary drugs in small streams in the European Union by liquid chromatography high resolution mass spectrometry. *Sci Total Environ* 670:1204–1225.

Cordeiro RM, Rosa CM, da Silva RJB. 2018. Measurements recovery evaluation from the analysis of independent reference materials: Analysis of different samples with native quantity spiked at different levels. *Accredit Qual Assur* 23:57–71.

da Silva BF, Jelic A, López-Serna R, Mozeto AA, Petrovic M, Barceló D. 2011. Occurrence and distribution of pharmaceuticals in surface water, suspended solids and sediments of the Ebro River basin, Spain. *Chemosphere* 85:1331–1339.

Daughton CG, Ternes TA. 1999. Pharmaceuticals and personal care products in the environment: Agents of subtle change? *Environ Health Perspect* 107(Suppl 6):907–938.

de Weert J, Streminska M, Hua D, Grotenhuis T, Langenhoff A, Rijnaarts H. 2010. Nonylphenol mass transfer from field-aged sediments and subsequent biodegradation in reactors mimicking different river conditions. *J Soils Sediments* 10:77–88.

Deutsche Industrienorm. 1987. 38409-2. German standard methods for the examination of water, waste water and sludge; parameters characterizing effects and substances (group H); determination of filterable matter and the residue on ignition (H 2). Berlin, Germany.

Eggleton J, Thomas KV. 2004. A review of factors affecting the release and bioavailability of contaminants during sediment disturbance events. *Environ Int* 30:973–980.

Eichbaum K, Brinkmann M, Buchinger S, Reifferscheid G, Hecker M, Giesy JP, Engwall M, van Bavel B, Hollert H. 2014. In vitro bioassays for detecting dioxin-like activity—Application potentials and limits of detection, a review. *Sci Total Environ* 487:37–48.

Escher BI, Dutt M, Maylin E, Tang JYM, Toze S, Wolf CR, Lang M. 2012. Water quality assessment using the AREc32 reporter gene assay indicative of the oxidative stress response pathway. *J Environ Monit* 14:2877–2885.

Escher BI, van Daele C, Dutt M, Tang JY, Altenburger R. 2013. Most oxidative stress response in water samples comes from unknown chemicals: The need for effect-based water quality trigger values. *Environ Sci Technol* 47:7002–7011.

Escher BI, Aït-Aïssa S, Behnisch PA, Brack W, Brion F, Brouwer A, Buchinger S, Crawford SE, Du Pasquier D, Hamers T, Hettwer K, Hilscherová K, Hollert H, Kase R, Kienle C, Tindall AJ, Tuerk J, van der Oost R, Vermeirssen E, Neale PA. 2018a. Effect-based trigger values for in vitro and in vivo bioassays performed on surface water extracts supporting the environmental quality standards (EQS) of the European water framework directive. *Sci Total Environ* 628–629:748–765.

Escher BI, Glauch L, König M, Mayer P, Schlichting R. 2019. Baseline toxicity and volatility cutoff in reporter gene assays used for high-throughput screening. *Chem Res Toxicol* 32:1646–1655.

Escher BI, Neale PA, Villeneuve DL. 2018b. The advantages of linear concentration-response curves for in vitro bioassays with environmental samples. *Environ Toxicol Chem* 37:2273–2280.

European Environment Agency. 2019. The European environment—State and outlook 2020: Knowledge for transition to a sustainable Europe. European Union, Luxembourg.

Gasperi J, Garnaud S, Rocher V, Moilleron R. 2008. Priority pollutants in wastewater and combined sewer overflow. *Sci Total Environ* 407: 263–272.

Gasperi J, Garnaud S, Rocher V, Moilleron R. 2009. Priority pollutants in surface waters and settleable particles within a densely urbanised area: Case study of Paris (France). *Sci Total Environ* 407:2900–2908.

Glaser C, Zarfl C, Rügner H, Lewis A, Schwientek M. 2020. Analyzing particle-associated pollutant transport to identify in-stream sediment processes during a high flow event. *Water* 12:1794.

Helsel DR. 1990. Less than obvious-statistical treatment of data below the detection limit. *Environ Sci Technol* 24:1766–1774.

Jordan P, Cassidy R. 2011. Assessing a 24/7 solution for monitoring water quality loads in small river catchments. *Hydrol Earth Syst Sci* 15: 3093–3100.

Karickhoff SW. 1981. Semi-empirical estimation of sorption of hydrophobic pollutants on natural sediments and soils. *Chemosphere* 10:833–846.

Kasprzyk-Hordern B, Dinsdale RM, Guwy AJ. 2009. Illicit drugs and pharmaceuticals in the environment—Forensic applications of environmental data, Part 2: Pharmaceuticals as chemical markers of faecal water contamination. *Environ Pollut* 157:1778–1786.

Kayhanian M, Singh A, Meyer S. 2002. Impact of non-detects in water quality data on estimation of constituent mass loading. *Water Sci Technol* 45:219–225.

Kim U-J, Oh JK, Kannan K. 2017. Occurrence, removal, and environmental emission of organophosphate flame retardants/plasticizers in a wastewater treatment plant in New York State. *Environ Sci Technol* 51: 7872–7880.

Kodešová R, Kočárek M, Kodeš V, Drábek O, Kozák J, Hejtmánková K. 2011. Pesticide adsorption in relation to soil properties and soil type distribution in regional scale. *J Hazard Mater* 186:540–550.

König M, Escher BI, Neale PA, Krauss M, Hilscherová K, Novák J, Teodorović I, Schulze T, Seidensticker S, Hashmi MAK. 2017. Impact of untreated wastewater on a major European river evaluated with a combination of in vitro bioassays and chemical analysis. *Environ Pollut* 220:1220–1230.

Kruve A, Leito I, Herodes K. 2009. Combating matrix effects in LC/ESI/MS: The extrapolative dilution approach. *Anal Chim Acta* 651:75–80.

Lee J, Bang K, Ketchum L Jr, Choe J, Yu M. 2002. First flush analysis of urban storm runoff. *Sci Total Environ* 293:163–175.

Lepom P, Brown B, Hanke G, Loos R, Quevauviller P, Wollgast J. 2009. Needs for reliable analytical methods for monitoring chemical pollutants in surface water under the European water framework directive. *J Chromatogr A* 1216:302–315.

Li JY, Tang JYM, Jin L, Escher BI. 2013. Understanding bioavailability and toxicity of sediment-associated contaminants by combining passive sampling with in vitro bioassays in an urban river catchment. *Environ Toxicol Chem* 32:2888–2896.

Madoux-Humery A-S, Dorner S, Sauvé S, Aboulfadl K, Galarneau M, Servais P, Prévost M. 2013. Temporal variability of combined sewer overflow contaminants: Evaluation of wastewater micropollutants as tracers of fecal contamination. *Water Res* 47:4370–4382.

Mateos R, Oliveira CM, Díez-Pascual AM, Vera-López S, San Andrés MP, da Silva RJB. 2020. Impact of recovery correction or subjecting calibrators to sample preparation on measurement uncertainty: PAH determinations in waters. *Talanta* 207:120274.

Meyer J, Bester K. 2004. Organophosphate flame retardants and plasticisers in wastewater treatment plants. *J Environ Monit* 6:599–605.

Müller A-K, Leser K, Kämpfer D, Riegraf C, Crawford SE, Smith K, Vermeirssen E, Buchinger S, Hollert H. 2019. Bioavailability of estrogenic compounds from sediment in the context of flood events evaluated by passive sampling. *Water Res* 161:540–548.

Müller ME, Escher BI, Schwientek M, Werneburg M, Zarfl C, Zwiener C. 2018. Combining in vitro reporter gene bioassays with chemical analysis to assess changes in the water quality along the Ammer River, Southwestern Germany. *Environ Sci Eur* 30:20.

Müller ME, Werneburg M, Glaser C, Schwientek M, Zarfl C, Escher BI, Zwiener C. 2020. Influence of emission sources and tributaries on the spatial and temporal patterns of micropollutant mixtures and associated effects in a small river. *Environ Toxicol Chem* 39:1382–1391.

Neale PA, Altenburger R, Aït-Aïssa S, Brion F, Busch W, de Aragão Umbuzeiro G, Denison MS, Du Pasquier D, Hilscherová K, Hollert H. 2017. Development of a bioanalytical test battery for water quality monitoring: Fingerprinting identified micropollutants and their contribution to effects in surface water. *Water Res* 123:734–750.

Neale PA, Braun G, Brack W, Carmona E, Gunold R, König M, Krauss M, Liebmann L, Liess M, Link M, Schäfer RB, Schlichting R, Schreiner VC, Schulze T, Vormeier P, Weisner O, Escher BI. 2020. Assessing the mixture effects in in-vitro bioassays of chemicals occurring in small agricultural streams during rain events. *Environ Sci Technol* 54:8280–8290.

Peter KT, Hou F, Tian Z, Wu C, Goehring M, Liu F, Kolodziej EP. 2020. More than a first flush: Urban creek storm hydrographs demonstrate broad contaminant pollutographs. *Environ Sci Technol* 54:6152–6165.

Phillips P, Chalmers A, Gray J, Kolpin D, Foreman W, Wall G. 2012. Combined sewer overflows: An environmental source of hormones and wastewater micropollutants. *Environ Sci Technol* 46:5336–5343.

Ruff M, Mueller MS, Loos M, Singer HP. 2015. Quantitative target and systematic non-target analysis of polar organic micro-pollutants along the river Rhine using high-resolution mass-spectrometry–identification of unknown sources and compounds. *Water Res* 87:145–154.

Schwarzenbach RP, Gschwend PM, Imboden DM. 2016. *Environmental Organic Chemistry*. John Wiley & Sons, Hoboken, NJ, USA.

Spahr S, Teixidó M, Sedlak DL, Luthy RG. 2020. Hydrophilic trace organic contaminants in urban stormwater: Occurrence, toxicological relevance, and the need to enhance green stormwater infrastructure. *Environ Sci Water Res* 6:15–44.

Szöcs E, Brinke M, Karaoglan B, Schäfer RB. 2017. Large scale risks from agricultural pesticides in small streams. *Environ Sci Technol* 51: 7378–7385.

Tran NH, Reinhard M, Khan E, Chen H, Nguyen VT, Li Y, Goh SG, Nguyen QB, Saeidi N, Gin KY-H. 2019. Emerging contaminants in wastewater, stormwater runoff, and surface water: Application as chemical markers for diffuse sources. *Sci Total Environ* 676:252–267.

US Environmental Protection Agency. 2000. Guidance for data quality assessment: Practical methods for data analysis. EPA QA/G-9 (QA00 update). Washington, DC.

van Gils J, Posthuma L, Cousins IT, Brack W, Altenburger R, Baveco H, Focks A, Greskowiak J, Kühne R, Kutsarova S. 2020. Computational material flow analysis for thousands of chemicals of emerging concern in European waters. *J Hazard Mater* 397:122655.

Villagrasa M, Guillamón M, Eljarrat E, Barceló D. 2007. Matrix effect in liquid chromatography–electrospray ionization mass spectrometry analysis of benzoxazinoid derivatives in plant material. *J Chromatogr A* 1157: 108–114.

Worrall F, Parker A, Rae J, Johnson A. 1996. Equilibrium adsorption of isoproturon on soil and pure clays. *Eur J Soil Sci* 47:265–272.

Zgheib S, Moilleron R, Saad M, Chebbo G. 2011. Partition of pollution between dissolved and particulate phases: What about emerging substances in urban stormwater catchments? *Water Res* 45:913–925.

